Thermochimica Acta 707 (2022) 179084

Contents lists available at ScienceDirect

Thermochimica Acta

journal homepage: www.elsevier.com/locate/tca

Short communication

High throughput optimization procedure to characterize vitrification kinetics

Anabella A. Abate [1,a], Daniele Cangialosi [*,b], Simone Napolitano [a,*]

[a] Laboratory of Polymer and Soft Matter Dynamics, Experimental Soft Matter and Thermal Physics (EST), Universite Libre de Bruxelles (ULB) Bruxelles 1050 Belgium
[b] Centro de Fisica de Materiales (CSIC-UPV/EHU), Paseo Manuel de Lardizabal 5, San Sebastian, 20018, Spain

ARTICLE INFO

Keywords:
FSC
Glass transition
Physical aging

ABSTRACT

We present VITRIFAST, a high throughput optimization procedure to characterize the vitrification kinetics based on calorimetric measurements. By analyzing the temperature dependence of specific heat capacity, the method determines the fictive temperature, T_f, and the enthalpy change during physical aging, ΔH, within only a few seconds. We tested VITRIFAST on the low molecular weight glass-former *o* – terphenyl (OTP) and on an archetypal glass forming polymer, polystyrene (PS), by analyzing the outcome of two classical sets of experiments. By means of fast scanning calorimetry (FSC), we characterized the vitrification kinetics in a wide range of cooling rates and the isothermal physical aging after vitrification at a given rate. In less than 3 minutes, our method could process 18 different calorimetric scans and provided values of T_f and ΔH in excellent agreement with those reported in the literature. VITRIFAST can be employed in the analysis of the temperature dependence of any type of second order derivative of free energy and represents a tremendous advance in the data analysis of calorimetric scans. The method is particularly helpful for fast scanning calorimetry users, considering the extremely large number of heat capacity scans recorded by this technique within a few minutes.

1. Introduction

Vitrification is a complex phenomenon ubiquitously encountered in systems where crystallization is avoided, for instance by fast cooling [1,2]. It entails the transformation (glass transition) from the metastable supercooled liquid into a glass, whose signature is a kink in first order thermodynamic properties (volume, enthalpy, entropy). The non-equilibrium nature of a glass underlines the kinetic nature of vitrification. As a result, glasses always experience an evolution toward an equilibrium thermodynamic state. This equilibration kinetics results in a time dependent loss of the excess in first order thermodynamic properties, a phenomenon known as structural recovery [3] or physical aging [4,5].

Characterizing the glass transition and physical aging by calorimetric methods, such as differential scanning calorimetry (DSC), is widespread in the laboratory practice. This class of techniques delivers the specific heat, that is, the first derivative at constant pressure of enthalpy. Since the glass transition is underlined by a kink in the temperature dependence of enthalpy, a step in the specific heat is observed in DSC [6]. The glass transition temperature, T_g, is conventionally obtained from the mid-point of the step or the temperature of maximum inflection of the specific heat. Apart from their arbitrary nature, these methods often fail to provide satisfactory and physically meaningful values of T_g, especially when the glass transition encompasses a broad temperature interval. Furthermore, methods based on the analysis of the step in the specific heat suffer from the drawback that only a limited range of cooling/heating rates can be explored. At small rates the detection of the step in the specific heat might fall beyond the instrumental limit. On the opposite extreme, high rates may result in serious non-homogeneous thermal lags throughout the sample [7–9], which generally prevents a precise characterization of both T_g and width of the glass transition.

A way to attain a well-defined characterization of vitrification relies on the concept of fictive temperature, T_f, long ago introduced by Tool [10]. T_f is defined as the intersection of the glass line, drawn from the thermodynamic state of a glass with the melt line, see scheme in Fig. 1 left panel. The so-defined T_f, evaluated on a glass vitrified upon cooling and re-heated at the same rate, is within a few Kelvin equal to the T_g

* Corresponding author.
E-mail addresses: daniele.cangialosi@ehu.eus (D. Cangialosi), snapolit@ulb.ac.be (S. Napolitano).
[1] Current affiliation: Department of Physics. Instituto de Física del Sur (IFISUR), Consejo Nacional de Investigaciones Científicas y Tecnicas (CONICET), Universidad Nacional del Sur, 8000 Bahia Blanca, Argentina

https://doi.org/10.1016/j.tca.2021.179084
Received 6 September 2021; Received in revised form 27 October 2021; Accepted 28 October 2021
Available online 2 November 2021

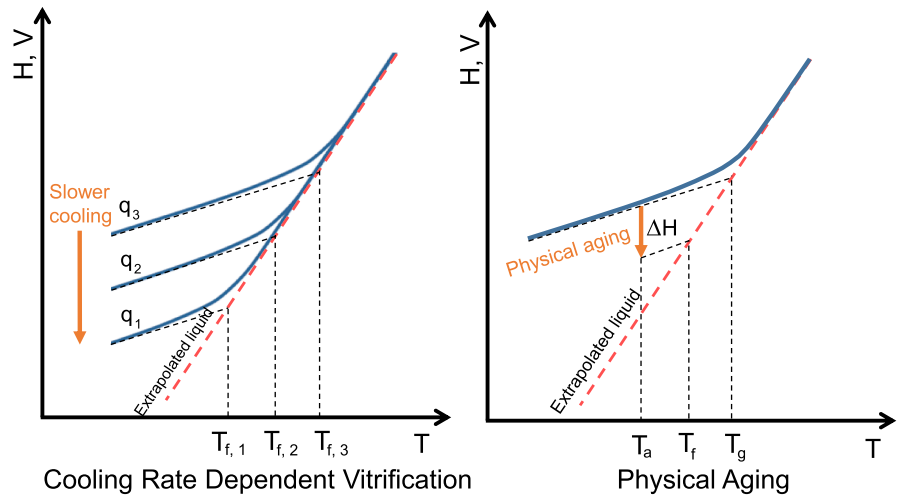

Fig. 1. Schematic representation of how T_f is defined in experiments where vitrification kinetics as a function of the cooling rate is characterized (left panel) and those based on isothermal physical aging below T_g (right panel).

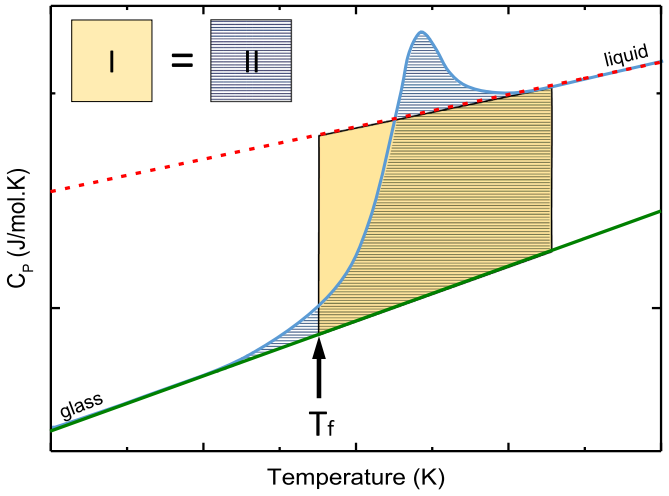

Fig. 2. Scheme of the Moynihan method employed to obtain T_f from the calculation of the areas I and II of the aged curve (blue line). The green and the red lines represent the glass and liquid lines, respectively. (For interpretation of the references to colour in this figure legend, the reader is referred to the web version of this article.)

taken from the mid-point of the specific heat step [11]. Importantly, T_f can be determined over a wide range of cooling rates, provided the employment, after cooling, of a fixed heating rate adequate to have a measurable heat flow rate and minimizing thermal lag. In such a way, combining different calorimetric methods, vitrification kinetics in terms of T_f can be characterized over a wide range of cooling rates and annealing time scales [8,12–17]. Furthermore, T_f is a reliable parameter quantifying the thermodynamic state attained after a given thermal protocol, as for example for a glass formed at a given rate and aged at a given temperature, T_a, see scheme in Fig. 1 right panel [18,19]. In this case, apart from and in connection to T_f, the enthalpy reduction, ΔH, taking place during aging can also be quantified.

Operationally, the determination of the fictive temperature of a glass with a given thermodynamic state must account for the fact that calorimetry measures the specific heat, rather than the enthalpy. Hence, the so-called Moynihan or the matching-area method is employed to determine T_f based on second order thermodynamic properties [20]. The method is visually presented in Fig. 2. T_f is determined by identifying the temperature obeying to the following property: the area included between the melt and glass specific heat matches the area included between the experimental and the glass specific heat. This procedure mathematically reads:

$$\int_{T_f}^{T>>T_g} (c_{pm} - c_{pg})dT = \int_{T<<T_g}^{T>>T_g} (c_p - c_{pg})dT, \quad (1)$$

where c_{pm} and c_{pg} are the supercooled melt and glass specific heats, respectively.

For a single measurement the employment of the Moynihan method does not present mayor challenges and the only concern regards the correct choice of the glass and liquid lines; see Fig. 2. In contrast, it is usually necessary to determine the value of T_f in a consistent way for a set of specific heat scans, for instance in cooling rate dependent determination of T_f or in isothermal aging experiments at different times. In this case, a precise determination of T_f is challenged by the baseline mismatch among different scans. The procedure permitting to realign the calorimetric scans is done as schematically depicted in Fig. 3 by changing the slope (panel a)) and vertically shifting (panel b)) a given c_p scan (blue line) to a reference curve c_p^{ref} (dashed orange line). This set of

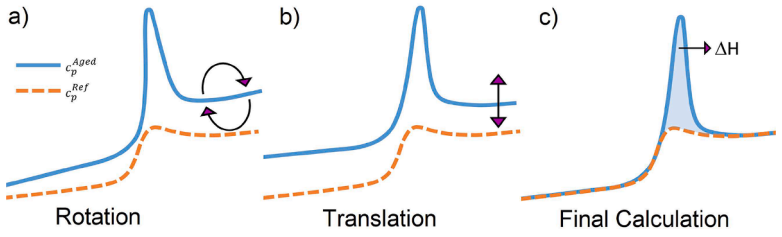

Fig. 3. Transformations to the aged measurement $c_p^{Aged}(T)$: a) change of slopes and b) vertical shift to obtain $c_p^{New}(T)$ that overlap with $c_p^{Ref}(T)$ for temperatures below and above the glass transition.

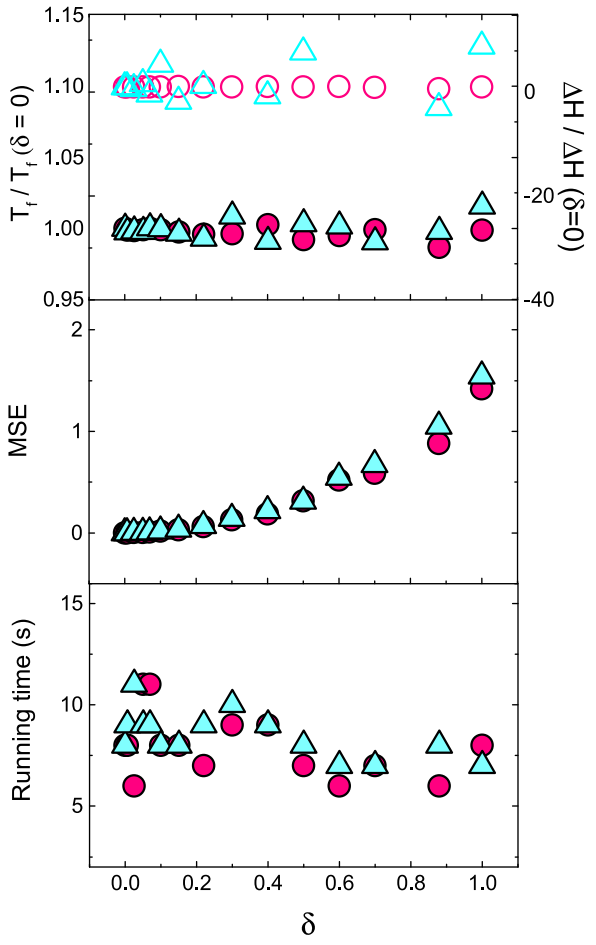

Fig. 4. Impact of the noise artificially added to the calorimetric scans to the values of the fictive temperature T_f (closed symbols) and the recovered enthalpy ΔH (open symbols) normalized by its values at zero noise. Two limiting cooling rates were considered, pink circles 2000 K/s, cyan triangles 0.1 K/s. The MSE and the running time are also reported (For interpretation of the references to color in this figure legend, the reader is referred to the web version of this article).

operations aims at superposing the glass and melt lines of a given set of c_p scans to the reference curve. If the superposition is manually performed for each scan, the determination of T_f can be highly tedious and time consuming.

The same line of reasoning applies to the determination of the amount of recovered enthalpy in physical aging experiments, see Fig. 1 right panel. From the connection of the specific heat to the enthalpy, this is done integrating the area underlined between the aged curve and the reference, that is, the scan corresponding to the as-just quenched glass, see Fig. 3 panel c). Hence, the recovered enthalpy is computed as:

$$\Delta H = \int_{T_{min}}^{T_{max}} \left(c_p(T) - c_p^{Ref}(T) \right) dT \tag{2}$$

where, $T_{\min}$ and $T_{\max}$ are the temperatures including the range where enthalpic effect are present. As for T_f, also in this case a well-defined characterization of ΔH requires the superposition of all glass and liquid lines to those of the reference, that is, the specific heat scan corresponding to zero aging time, obtained heating a glass immediately after cooling.

With the aim of expediting the procedure schematized in Fig. 3, in this study, we introduce VITRIFAST, a robust method which provides, within only a few seconds, the fictive temperature and the recovered enthalpy from calorimetric measurements. Our method is highly suitable for investigation of the glass transition and physical aging by fast scanning calorimetry, an experimental approach capable to measure a tremendously large number of heat capacity scans within few minutes.

2. Methods

The first step to quantitatively analyze a vitrification kinetics experiment (determine the fictive temperature, T_f, and the amount of recovered entalpy, ΔH) consists in verifying that the aged and reference curves overlap for temperatures below and above the glass transition range, as shown in Fig. 1c). As soon as such condition is achieved, we can further analyze the calorimetric data by means of the Moynihan method. We remark that, while in the following text we will refer to the specific heat capacity, the same data processing can be applied to heat flow rate scans. The determination of the fictive temperature, in fact, does not require knowing the sample mass.

First, we define the model function that we will use to perform the optimization procedure:

$$c_p^{New}(a,b,T) = S(a,T).c_p^{Aged}(T) + b \tag{3}$$

In this model, $c_p^{Ref}(T)$ and $c_p^{Aged}(T)$ are the specific heat values as measured for the reference and the aged samples. We indicate with $c_p^{New}(T)$ the correction of $c_p^{Aged}(T)$ after the execution of our optimization procedure. VITRIFAST follows the same strategy commonly used in the analysis of calorimetric scans, consisting in the adjustment of two parameters, a and b.

Our method permits to significantly reduce the time required to obtain those parameters in a reliable way. By introducing the constant b quantifying a vertical translation (see Fig. 1 b)), we can compute the function $S(a,T)$ that accounts for the change in slope of the aged curve (see Fig. 1 a)), as:

$$S(a,T) = \frac{A(a).c_p^{Aged}(T) - A(a).T_{max} + c_p^{Aged}(T_{max})}{c_p^{Aged}(T_{max})} \tag{4}$$

where $A(a) = \frac{(1-a/c_p^{Aged}(T_{\min}))}{\Delta T}$, $\Delta T = T_{final} - T_{initial}$, with $T_{initial}$ and T_{final} the initial and the final temperatures of the experiment, respectively. $T_{\min}$ and $T_{\max}$ are the temperatures that delimit the temperature ranges to superpose aged curves to the reference. Specifically, $T_{\min}$ ($T_{\max}$) is the temperature below (above) which the aged scan must overlap with the reference scan, that is, where non-reversing effects due to the glass transition are not present.

For the optimization procedure we employ least-squares fitting, implemented via Python with SciPy. The latter is an open-source scientific computing library for the Python programming language, and least-squares fitting is a well-known statistical technique to estimate parameters in mathematical models. It concerns finding the minimum of a function, in our case $F(a,b,T)$, defined as:

$$F(a,b,T) = \sum_{i=0}^{N} \rho(f_i(a,b,T))^2, \tag{5}$$

where N is the number of available data points in the calorimetric scan $c_p(T)$, measured from the initial temperature, $T_{initial}$, to the final temperature, T_{final}; ρ is a loss function filtering the data in the temperature range where the glass transition occurs (in our case from $T_{\min}$ to $T_{\max}$). Finally, $f_i(a,b,T)$ is the $i-th$ component of the vector of residuals, which here corresponds to the difference between the model prediction of the new corrected specific heat, $c_p^{New}(T)$, and the reference data, $c_p^{Ref}(T)$, for all the experimental points $N = \{(N_i)|i = T_{initial},\ldots,T_{end}\}$, and is defined as:

$$f_i(a,b,T) = c_p^{New}(a,b,T) - c_p^{Ref}(T) \tag{6}$$

Our optimization procedure consists in the minimization of Eqn. 5.

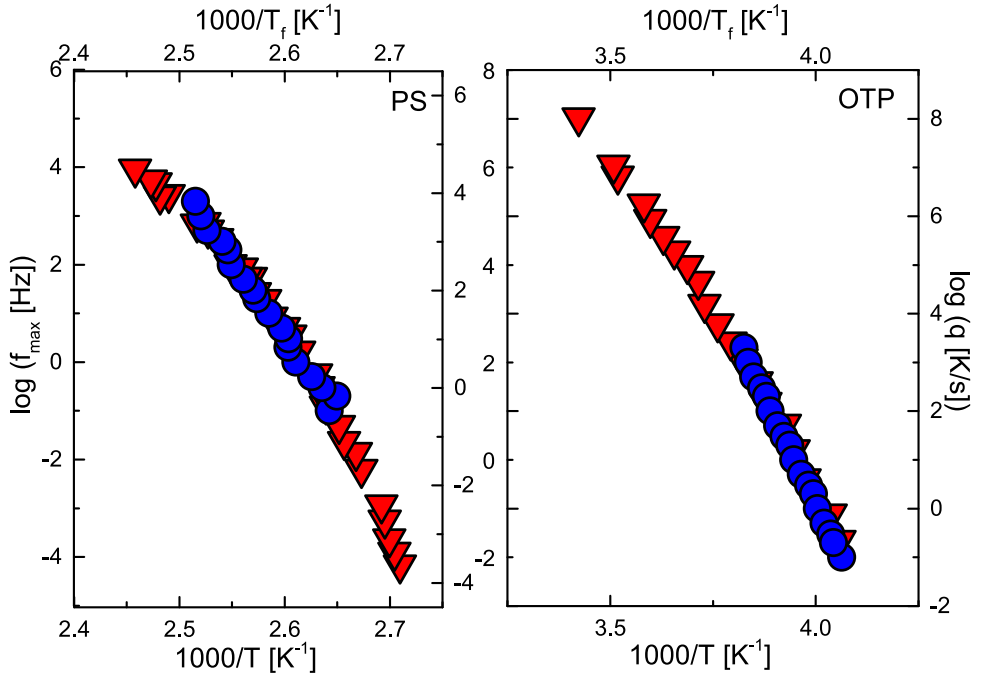

Fig. 5. Comparison of the cooling rate dependence of the fictive temperature obtained in the present work (blue circles) and the temperature dependence of the relaxation rate (red triangles), for PS (left panel) and OTP (right panel), taken from refs[12,21]. (For interpretation of the references to colour in this figure legend, the reader is referred to the web version of this article.)

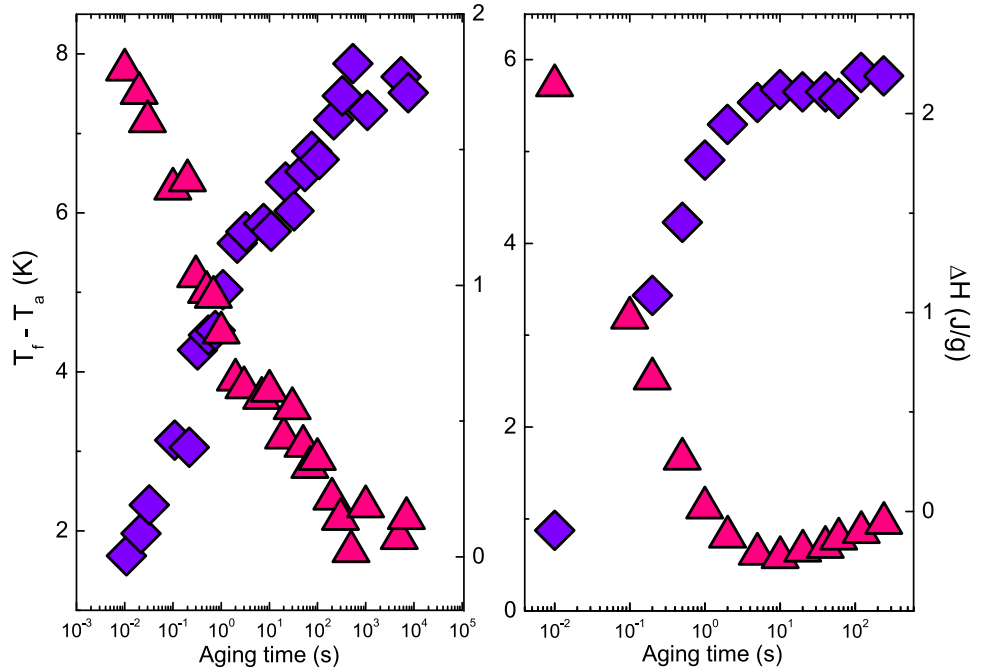

Fig. 6. Aging time evolution of ΔH (violet diamonds) and of the distance of TT_f from the aging temperature (pink triangles) for PS (left panel) and OTP (right panel) samples, aged 5 K below T_f(1000 K/s) (For interpretation of the references to color in this figure legend, the reader is referred to the web version of this article).

From a physical viewpoint, this procedure corresponds to minimizing the difference between the corrected specific heat, $c_p^{New}(T)$, and the reference, $c_p^{Ref}(T)$, for temperatures much below and above the glass transition, where non-reversing effects are not present and, therefore, those two curves must overlap as shown in Fig. 3 c).

This optimization has hitherto been tedious and time-consuming, as it requires manually changing the values of a and b, often via a hit-and-try procedure followed by evaluation, either by eye or via more sophisticated analytical methods. VITRIFAST provides an automatized solution of the optimization problem of Eqn. 3 using the models of Eqn. 1 and 2. This procedure requires a very short computation time: only a few seconds are necessary to obtain the parameters a and b for each c_p scan. After obtaining $c_p^{New}(T)$, the determination of the recovered enthalpy, ΔH, is straightforward. Please note that in the latter case it is necessary to know the mass of the sample.

Obtaining the fictive temperature, T_f, via the matching-areas method

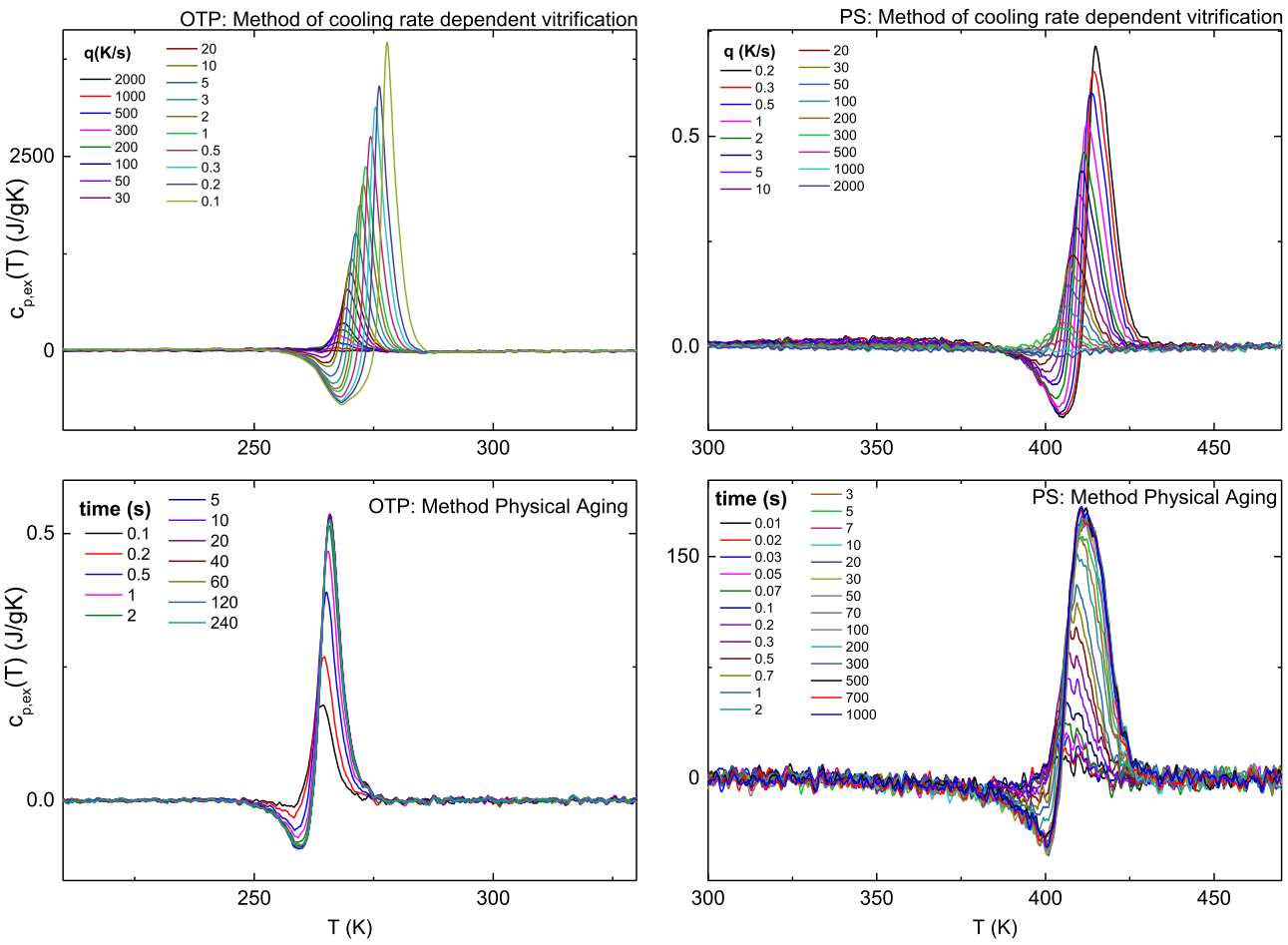

Fig. 7. $c_{p,ex}(T)$ of $o-$ terphenyl (OTP) and polystyrene (PS) after running the ML-based code for the two vitrification methods analyzed: Cooling Rate Dependent Vitrification, upper panels, and Physical Aging, bottom panels.

showed in Fig. 2, requires a further step, as this method relies on the description of the glass and liquid specific heats. Therefore, we implemented our method in Phyton using the Linear Regression, Numpy and Scipy libraries. First, we automatically fit two linear curves for the reference curve in the liquid and glassy state, $c_p^{liquid}(T)$ and $c_p^{glass}(T)$ in the range $T > T_{melt}$ and $T < T_{glass}$, respectively, as shown in Fig. 2. Here, T_{melt} (T_{glass}) is the temperature above (below) which a linear fit to the melt (glass) line can be performed, with no interference of non-reversing effects due to the glass transition. Importantly, T_{melt} e T_{glass} generally differ from $T_{\max}$ and $T_{\min}$. The former, in fact, generally encompass larger temperature ranges than the former, as the melt and glass lines are traced on the reference curve where non-reversing effects are minimized. Subsequently, using the Simpsons rule we compute the area below the melt and the glass specific heat in a temperature range from $T_{\min}$ (T_{on}) up to $T_{\max}$. Simultaneously, we compute the area between $c_p^{New}(T)$ and $c_p^{glass}(T)$ in the range $T_{\min}$ to $T_{\max}$. T_f is determined as the temperature satisfying the equivalence indicated by Eqn. 1. In order to numerically solve this expression, we implemented a loop which varies T_f from $T_{\min}$ to $T_{\max}$ with a (tunable) increment of 0.005 K.

3. Results

In order to evaluate the robustness of the method, we tested its precision in the case of noisy calorimetric scans, obtained by adding white noise to a standard data set obtained via FSC. We define the noise ratio as δ:

$$\delta = \frac{\varepsilon}{c_{p,ex}} \tag{7}$$

where ε is the amplitude of the added random white noise to the specific heat curves with an amplitude of approximately $\sim 3\sigma$, and $c_{p,ex} = c_p^{liquid}(T_{\max}) - c_p^{glass}(T_{\min})$ is the difference of the specific heat in the liquid and the glassy state (see Supplementary Information). For this purpose it is convenient to calculate the mean of the squares of the residuals, that is, the mean squared displacement (MSE), defined as:

$$MSE = \frac{1}{N}\sum_{i=1}^{N}(f_i(a,b,T))^2 \tag{8}$$

Fig. 4 shows the evolution of the obtained parameters T_f, ΔH, MSE and the execution time after running our method for data with increasing noise δ (from 0 to 1). Note that the outputs of the method differ with respect to the zero noise in less than 10 % for δ values until $\delta = 0.4$.

To prove the efficiency of the method, we also analyzed heat capacity scans of the low molecular weight glassformer $o-$ terphenyl (OTP) and polystyrene (PS, Mw = 311,000) obtained by FSC. Two sets of experiments were performed. In the first set (Cooling Rate Dependent Vitrification, Fig. 1 left panel), samples were heated at 1000 K/s immediately after vitrification at cooling rates (q) between 4000 K/s and 0.1 K/s. This is a classical experiment that provides the cooling rate dependence of the fictive temperature. Importantly, following the Frenkel-Kobeko-Reiner equation ($q\tau$=const) [12], the outcome of these calorimentric experiments (T_f, q) is directly related to relaxation data in isothermal

conditions (T, τ^{-1}), where τ is the timescale of spontaneous fluctuations.

We compared the variation of log q vs. $1000/T_f$ for the obtained values of T_f with log f_{max} vs. 1000/T for measurements done via broadband dielectric spectroscopy and AC-calorimetry [12,21]; please note that $2\pi f_{max}\tau = 1$. Fig. 5 shows that the outcome of our analysis is in excellent agreement with the relaxation data, verifying the efficiency of our method.

In a second set of experiments (Physical Aging, Fig. 1 right panel), we measured the change in the fictive temperature of samples of OTP and PS as a function of the aging time in isothermal conditions. In such experiments, the distance from T_f and the aging temperature, T_a saturates to a constant value after long aging times. In particular, for PS $T_f - T_a$ evolves from 8 to 2 K within 10^2, while for OTP it goes from 6 to 1 K within 10^4. A correlated trend is observed also for the recovered entalpy (ΔH). The long time T_f limit for OTP coincides within 1 K with the aging temperature, indicating that, within experimental errors, the supercooled liquid line has been reached. Regarding PS, a minor mismatch between the long aging time T_f and T_a can be observed. The difference between the two materials can be explained considering the thermal lag [7,8]. Indeed, the mass of PS employed in our experiments was about 200 ng, that justifies a 2 K thermal lag [7]; in contrast, the mass of our OTP sample was smaller than 100 ng, resulting in an almost zero (1 K) thermal lag [7]. Our results for PS in terms of time scale to reach equilibrium are generally in accordance with previous physical aging results on the same polymer by FSC [22]. As a showcase for PS, a plot of the same quantity as in Fig. 6, without the optimization of the glass and melt lines prior to the application of the Moynihan method, is given in the SI. This shows that without running the optimization protocol the aging time evolution of T_f appears highly scattered, thus demonstrating that strength of our method in delivering physically sound results.

Finally, $c_{p,ex}(T)$ defined as $c_p^{New}(T) - c_p^{Ref}(T)$ was analyzed for all sets of experiments after the execution of our optimization procedure. Fig. 7 shows that the baseline after the difference is constant and equal to zero for all the cases, indicating the high performance of our method.

4. Conclusion

In conclusion, we introduce VITRIFAST, an optimization procedure capable to extract parameters like the fictive temperature T_f and the recovered enthalpy ΔH from calorimetric scans, in a fast and efficient way. The code, made available for all the users, tremendously speeds up the analysis of typical vitrification kinetics experiments. Tens of scans can be processed within just a few minutes. Finally, we stress that the advantages of employing VITRIFAST are not limited to calorimetric scans. The method can be promptly applied to the analysis of the temperature dependence of second order derivative of the free energy and to any other data set where comparison between two baselines is required, as for instance in melting of crystals.

5. Code availability

The Phyton code used for the analysis is described in the Supporting Information together with some notes on its use. Further information on the method, its updates and access to the code are available at https://dynamics.ulb.be/vitrifast

CRediT authorship contribution statement

Anabella A. Abate: Data curation, Formal analysis, Investigation, Methodology, Writing – original draft. **Daniele Cangialosi:** Conceptualization, Data curation, Investigation, Methodology, Writing – original draft, Writing – review & editing. **Simone Napolitano:** Conceptualization, Data curation, Investigation, Methodology, Writing – original draft, Writing – review & editing.

Declaration of Competing Interest

None.

Acknowledgements

S. N and A. A. acknowledge financial support from Action Concert Recherche-ULB under project SADI, and the Fonds de la Recherche Scientifique FNRS under Grant T.0184.20 EXOTICAGE. D.C. acknowledges financial support from the project PGC2018-094548-B-I00 (MICINN-Spain and FEDER-UE) and the project IT-1175-19 (Basque Government)

Supplementary material

Supplementary material associated with this article can be found, in the online version, at doi:10.1016/j.tca.2021.179084.

References

[1] J.W.P. Schmelzer, I.S. Gutzow, Glasses and the glass transition, Wiley-VCH, Weinheim, 2011.
[2] S. Napolitano, E. Glynos, N.B. Tito, Glass transition of polymers in bulk, confined geometries, and near interfaces, Rep. Progr. Phys. 80 (3) (2017) 036602.
[3] A.J. Kovacs, Glass transition in amorphous polymers: a phenomenological study, Fortsch. Hochpolym. Fo. 3 (1/2) (1963) 394–508.
[4] L.C.E. Struik, Physical aging in amorphous polymers and other materials, Technische Hogeschool Delft. (1977).
[5] D. Cangialosi, V.M. Boucher, A. Alegria, J. Colmenero, Physical aging in polymers and polymer nanocomposites: recent results and open questions, Soft Matter 9 (2013) 8619–8630.
[6] B. Wunderlich, Thermal analysis of polymeric materials, Springer, Berlin, Heidelberg, 2005.
[7] J.E. Schawe, Measurement of the thermal glass transition of polystyrene in a cooling rate range of more than six decades, Thermochim Acta 603 (2015) 128–134.
[8] X. Monnier, A. Saiter, E. Dargent, Vitrification of pla by fast scanning calorimetry: towards unique glass above critical cooling rate? Thermochim. Acta 658 (2017) 47–54.
[9] K. Jariyavidyanont, A. Abdelaziz, R. Androsch, C. Schick, Experimental analysis of lateral thermal inhomogeneity of a specific chip-calorimeter sensor, Thermochim. Acta 674 (2019) 95–99.
[10] A. Tool, Relation between inelastic deformability and thermal expansion of glass in its annealing range, J. Am. Ceram. Soc 29 (9) (1946) 240–253.
[11] P. Badrinarayanan, W. Zheng, Q. Li, S.L. Simon, The glass transition temperature versus the fictive temperature, J. Non-Cryst. Sol 353 (26) (2007) 2603–2612.
[12] J.E.K. Schawe, Vitrification in a wide cooling rate range: the relations between cooling rate, relaxation time, transition width, and fragility, J. Chem. Phys 141 (18) (2014) 184905.
[13] T.V. Tropin, G. Schulz, J.W. Schmelzer, C. Schick, Heat capacity measurements and modeling of polystyrene glass transition in a wide range of cooling rates, J. Non-Cryst. Sol 409 (2015) 63–75.
[14] X. Monnier, D. Cangialosi, Thermodynamic ultrastability of a polymer glass confined at the micrometer length scale, Phys. Rev. Lett 121 (2018) 137801, https://doi.org/10.1103/PhysRevLett.121.137801.
[15] M.K. Saini, X. Jin, T. Wu, Y. Liu, L.M. Wang, Interplay of intermolecular interactions and flexibility to mediate glass forming ability and fragility: a study of chemical analogs, J. Chem. Phys 148 (12) (2018) 124504.
[16] J.E. Schawe, K.U. Hess, The kinetics of the glass transition of silicate glass measured by fast scanning calorimetry, Thermochim. Acta 677 (2019) 85–90.
[17] X. Monnier, D. Cangialosi, B. Ruta, R. Busch, I. Gallino, Vitrification decoupling from α-relaxation in a metallic glass, Sci. Adv 6 (17) (2020).Eaay1454
[18] I.M. Hodge, Enthalpy relaxation and recovery in amorphous materials, J. Non-Cryst. Sol. 169 (3) (1994) 211–266.
[19] D. Cangialosi, Dynamics and thermodynamics of polymer glasses, J. Phys.: Cond. Matt. 26 (15) (2014) 153101.
[20] C.T. Moynihan, P.B. Macedo, C.J. Montrose, P.K. Gupta, M.A. De Bolt, J.F. Dill, B. E. Dom, P.W. Drake, A.J. Eastel, P.B. Elterman, R.P. Moeller, H. Sasabe, J. A. Wilder, Structural relaxation in vitreous materials, Ann. NY Acad. Sci. 279 (1976) 15–35.OCT15
[21] G.P. Johari, M. Goldstein, Viscous liquids and the glass transition. ii. secondary relaxations in glasses of rigid molecules, J. Chem. Phys. 53 (6) (1970) 2372–2388, https://doi.org/10.1063/1.1674335.
[22] N.G. Perez-De-Eulate, D. Cangialosi, Double mechanism for structural recovery of polystyrene nanospheres, Macromolecules 51 (9) (2018) 3299–3307.